Proceedings of the 2nd International Conference on Green Energy, Environment and Sustainable Development (GEESD2021), D. Dobrotă and C. Cheng (Eds.)

doi:10.3233/ATDE210277

Pressure Drop Measurements and Simulations for the Protective Mesh Screen Before the Gas Turbine Compressor

L X NIE[a], Y YIN[b,1], L Y YAN[b] and S W ZHOU[c]
[a] *The 708th Research Institute of China State Shipbuilding Corporation, Shanghai 200000, China*
[b] *College of Power and Energy Engineering, Harbin Engineering University, Harbin 150000, China*
[c] *China Ship Research and Design Center, Wuhan 430000, China*

Abstract. This paper characterizes the pressure drop of incompressible airflow when passing by a metal mesh screen which acts as a protection from sucking foreign solid matters before the gas turbine compressor. The wire diameter is 1.2mm and the mesh number is 3. Two experiments are conducted in different time period of a day to guarantee the experimental repeatability. The experimental data are used in regression analysis to obtain a quadratic correlation between the pressure drop across the screen and the fluid velocity. Numerical simulations are utilized to investigate detailed velocity and pressure fields around the wires and the Standard k-ε turbulence model is used. The results show that the fluid suffers from around 140Pa and 250Pa total pressure drop at the velocity of 20m/s and 30m/s respectively. The pressure closely upstream of the wires is as high as 4 times of the inlet flow level, while wide negative pressure regions are observed downstream of the wires resulting from fluid stagnation, reverse flow and recirculation. The empirical correlation obtained in the paper has a high confidence level and can be used in calculating the overall pressure drop of the gas turbine air intake system.

Keywords. Gas turbine compressor, pressure drop measurements, mesh screen

1. Introduction

The wire meshes play an important role in the gas turbine intake system. On the one hand, the wire meshes act as filters against liquid droplets or aerosols to limit the occurrence of fouling, erosion, and corrosion in the compressor section [1] and they are often twisted together like woven fabrics and also exist in the form of multi-layer pad. On the other hand, there is a layer of protective mesh screen arranged just before the compressor, which not only prevents the foreign matter from hurting the compressor blades but also increases the uniformity of the inlet velocity field. The wire meshes generally present superior ability of filtering and shielding. However, the pressure drop across the wire mesh can be high. It is essential to make it clear for the pressure drop

[1] Corresponding Author, Y YIN, College of Power and Energy Engineering, Harbin Engineering University, Harbin 150000, China; Email: yinyue@hrbeu.edu.cn.

characteristics and nearby flow field details of the wire mesh, since excessive pressure drop before the compressor would lead to severe deterioration in engine performance.

El-Dessouky et al. [2] measured the pressure drop of a wire mesh mist eliminator from multi-stage flash desalination units using the vertical U-tube manometer. The wire diameter was in the range of 0.2-0.32mm. The results showed that the pressure drop per unit length increases linearly with the dry gas velocity. The correlation between the pressure drops and packing velocity, vapor velocity and wire diameter is summarized from the experimental data. Helsør and Svendsen [3] measured dry pressure drop of wire mesh demisters under different system pressure using differential pressure transmitter. The porosity of the tested wire mesh is in the range of 93.4% to 98.5%. They found that the pressure drop variation for all systems fitted well to a Hazen-Dupuit-Darcy type equation. Rahimi and Abbaspour [4] used commercial CFD code FLUENT to simulate the pressure drop in demister. The turbulence model selected was k–ε model. The inlet velocity ranges from 1 to 7 m/s. The numerical simulation results show about 14-21% deviation against experimental and empirical method. Brekke and Bakken [1] conducted experimental investigations on the performance of gas turbine inlet wire mesh filter under both dry and wet conditions. They observed significant pressure loss change after the filters being exposed to moisture. Setekleiv and Svendsen [5] experimentally studied the pressure drop characteristics with multiphase flow of six different wire mesh pads using a Fuji pressure transmitter. Janajreh et al. [6] carried out numerical simulations on the pressure drop across the demister made of metal wire meshes. The calculation model is about real industrial demister dimensions. The turbulence model selected was realizable k–ε turbulence model. The deviation of the numerical results from the experimental results is less than 12%. Sun et al. [7] put forward a new geometrical simplification method for wire mesh filters during numerical simulations on their pressure losses. The relative errors between the numerical results of their 2D simplified models and the original 3D models are less than 1.62%. They also studied the effect of wire diameter, layer spacing and mesh size on the pressure loss as the single-phase air flowing through the wire mesh pad. Standard k-ε model was adopted as turbulence model. Setekleiv and Svendsen [8] measured the dry pressure drop for 8 wire mesh pads with three fluid systems: one low pressure system using air and two high pressure systems using nitrogen and natural gas. Bussière et al. [9] experimentally investigated the correlation between the pressure loss (friction factor) and velocity (Reynolds number) on the system of woven metal screens being the friction inducer and water being the working fluid. These screens are usually used as filters in LV circuit breakers. And they equipped the test section with four static pressure transducers to measure the pressure drop. Okolo et al. [10] numerically studied the flow and turbulence characteristics upstream, downstream and within a single layer cylindrical woven wire mesh screen. The k-ε model shown good match with the experimental data in the turbulence study. Fluid flow reduction and turbulent intensity decay are found from the woven wire mesh screens. Fouad Azizi [11] conducted a large number of experimental measurements on the pressure drop of water through woven screen meshes and more than 200 data points that spans 60 different screen geometries with fraction open areas ranging from 0.21 to 0.84 were obtained. The maximum investigated Reynolds number is also as high as 10^4. The pressure values in front of and behind the screens are measured by two pressure transducers. Two universal correlations that corresponding to two different theories were derived. Wang et al. [12] developed an analytical model for calculating the fluid pressure drop through metal

wire screens without the need of experimental measurements or numerical simulations. The analytical model only considers the standardized parameters about pore structures. The model is validated in the Reynolds number range of 0.1-1000 under room-temperature and cryogenic fluids, presenting a mean absolute relative error of 23.0% against the data in previous literatures. Abou-Hweij and Azizi [13] numerically studied hydrodynamic characteristics including velocity and pressure fields of the flow crossing plain-woven wire meshes, which are used in chemical industry as static mixers. The turbulence model k-ω SST was selected to capture the vortices and recirculation in the vicinity of the screens although under laminar flow regime. The authors found pressure recovery in the downstream region of the screen at relatively high Reynolds numbers while this does not exist at low Reynolds numbers.

Unlike the wire mesh filters in the filtering unit of the intake system, the main target of the protective mesh screen is to keep out of solid matters and rectification. This paper focuses on the pressure drop characteristics of the protective mesh screen. Both experiments and numerical simulations are carried out to investigate the mathematical relationship between the pressure drop across the screen and the fluid velocity in the velocity range of 0m/s to 30m/s. Numerical simulations of flow field analysis are conducted in order to figure out the situation of momentum transport and the mechanism of energy dissipation around the wires. Backflow and vortices pairs downstream of the intersections of the wires are found to be the main source of pressure loss. The significant velocity magnitude difference between the downstream regions of the apertures and the interwoven wires also brings about pressure loss by introducing strong fluid momentum transport.

2. Experimental Apparatus

The tested metal mesh screen is displayed in figure 1 and it is sandwiched between two square channels whose size is 200mm*200mm. The low speed wind tunnel test system of mesh screen pressure drop characteristics is shown in figure 2 including the fluid path, sealing elements, inlet mass flow rate measuring section and pressure drop measuring section. The inlet mass flow rate is monitored by both lemniscate flowmeter and TSI anemometer. Pressure measuring points are set at the downstream and upstream of the tested screen using two TSI anemometers. The tested screen is trapped between two rubber blankets for sealing. To guarantee the accuracy and repeatability of the experiments, we conducted the pressure drop measurements both in the morning and afternoon and the two experiments are referred to EXP1 and EXP2 separately.

Figure 1. The metal mesh screen tested.

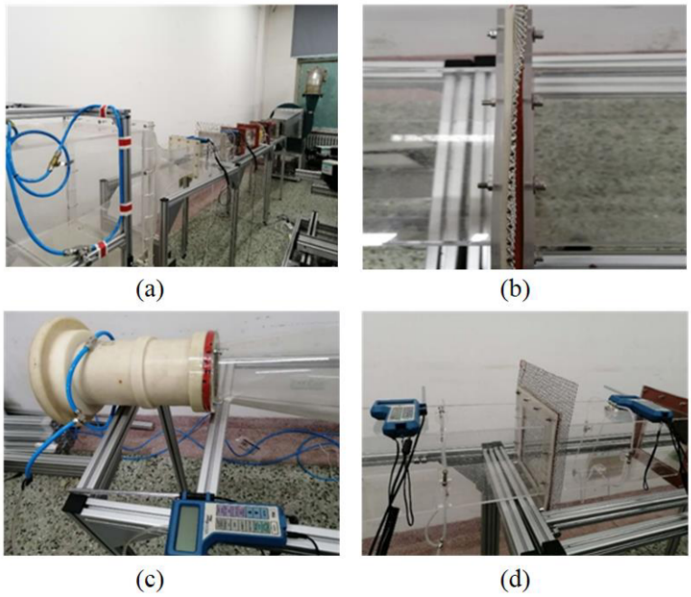

Figure 2. Layout of the experimental apparatus: (a) the fluid path structure; (b) sealing measures in the test system; (c) inlet mass flow rate monitoring; (d) monitoring the pressure drop across the protective mesh screen.

3. Computational Methods

3.1. Computational Domain

The function of the protective mesh screen just before the gas turbine compressor is shedding the foreign matters such as screws and debris from being absorbed into the compressor. Therefore, the mesh size is larger than the wire mesh filter for the convenience of air intaking. The mesh wires are cylindrical with their diameter being 1.2mm. The wires are interweaved at equal spacing. The aperture center-to-center distance is 6mm. The number of openings per inch is 3 (the mesh number is equal to 3), which means that the maximum particle diameter that can pass the wire mesh is 6.7mm. As shown in figure 3, the protective mesh screen is simplified to be a plain and periodic 3D model. The inlet and outlet are tailored to be 18mm×18mm cross section. The total length of the computational domain is 80mm. The velocity-inlet boundary conditions and pressure-outlet boundary conditions are imposed respectively on the inlet and outlet sections. And the lateral surfaces are set as periodic boundaries.

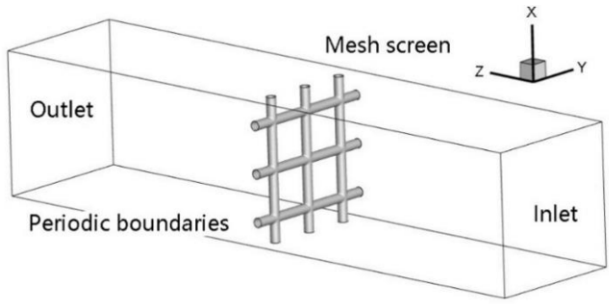

Figure 3. The computational domain of numerical simulations.

3.2. Computational Grids

The overall view of the computational grid is shown in figure 4a. The commercial software ICEMCFD was used to generate the unstructured tetrahedral grids. The magnified view of grids around the screen is shown in figure 4b. The mesh is refined with prism layers whose maximum height is 0.2mm around the screen surfaces. The grid independence study was performed to balance computational accuracy and efficiency. Three sets of grids were generated and their node numbers are 819,435, 1,013,916 and 1,844,555. The numerical results of the pressure coefficients along the front and back horizonal lines on the wire surface using the three sets of grids are shown in figure 5. And the definition expression of the pressure coefficient is as follows.

$$C_p = \frac{p - p_i}{0.5\rho_i v_i^2}$$

where p is local pressure, p_i is the free flow pressure, ρ_i is the free flow density and v_i is the free flow velocity.

It can be seen from the pressure coefficient distributions that the numerical results of 819,435 node number grids are irregular and inaccurate, while the results of 1,013,916 node number grids show the same changing trend and little difference with that of 1,844,555 node number grids. Therefore, the 1,013,916 node number grids are applied in the following numerical simulations.

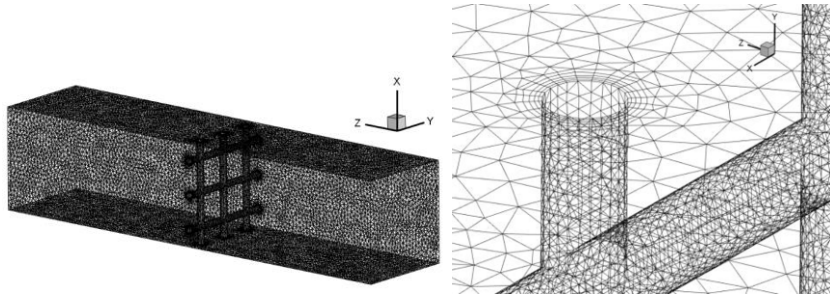

(a) (b)

Figure 4. Computational grid: (a) overall view; (b) magnified view of grids around the screen.

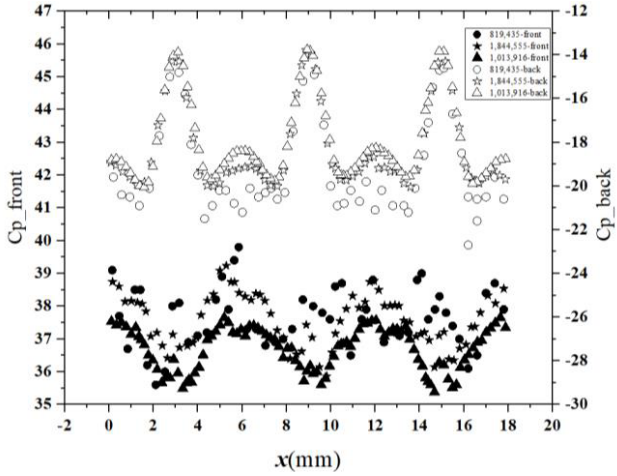

Figure 5. The pressure coefficient distribution on the front and back horizonal parallel lines of the wire surface.

3.3. Boundary Conditions and Solving Method

The protective mesh screen is equipped in marine gas turbine intake system in practice, the coming flow for it is generally stable filtered airflow. Steady state flow field and pressure drop characteristics are solved in numerical simulations. In the research of Janajreh et al. (2013) [6], the authors draw the conclusion that the k-ε turbulence models show better performance than the k-ω turbulence model and the transition models in predicting pressure drop characteristics of woven wire screens. In this paper Standard k-ε turbulence model is applied to carry out the subsequent calculations about the metal mesh screen. The SIMPLE algorithm is applied as the pressure-velocity coupling scheme. Second-order discretization schemes are utilized for the to-be-solved field variables. The convergence criteria are set as the residuals being less than 10-5. The fluid phase, air, is assumed to be ideal-gas. The air density is 1.225 kg/m^3 and the dynamic viscosity is 1.7894×10^{-5}kg/m·s. The gas velocity is set at the inlet from 1m/s to 30m/s, which conforms to the experimental conditions. Constant pressure of 1atm is imposed at the outlet. Periodic boundary conditions are imposed on the four sidewalls.

4. Results and Discussion

4.1. Pressure Drop Characteristics in Experiments

The mesh number of the current screen is 3. The data points about the relationship between the pressure drop and the velocity are obtained, which can reflect the performance of the protective mesh screen in the gas turbine air intake system. Since the channel sectional area remains unchanged and air density has little difference behind and in front of the tested screen, the pressure difference across the screen can be equivalent to the total pressure difference. Two experiments are conducted in two time periods of a day. The ambient temperature is 26.6°C and the atmospheric pressure is 99.02kPa for EXP1. The ambient temperature is 26.6°C and the atmospheric pressure is

99.05Pa for EXP2. The experimental data measured from EXP1 and EXP2 are listed in table 1. And average values of the pressure drop under the same velocity condition but at different moments are calculated in order to reduce experimental errors.

Table 1. Experimental data measured in EXP1 and EXP2.

Inlet velocity at the flowmeter (m/s)		**Velocity at the test section (m/s)**		**Total pressure drop (Pa)**	
EXP1	EXP2	EXP1	EXP2	EXP1	EXP2
9.03696	10.32796	2.55506	2.92007	3.0	3.0
12.90994	18.02776	3.65009	5.09707	5.5	9.5
18.61899	21.21320	5.26423	5.99770	11.5	12.5
22.36068	25.49510	6.32213	7.20834	16.5	20.0
27.68875	30.22141	7.82856	8.54463	25.0	25.5
33.14111	36.74235	9.37013	10.38832	36.0	40.0
39.05125	40.33196	11.04113	11.40323	50.5	48.0
43.39739	50.53052	12.26993	14.28671	63.0	73.0
49.07477	56.12486	13.87512	15.86843	79.5	90.5
55.07571	62.98148	15.57179	17.80703	101.5	117.0
62.44998	66.45801	17.65675	18.78996	124.5	125.5
67.33003	74.38638	19.03651	21.03158	140.0	159.0
	79.05694		22.35211		177.5
	83.16650		23.51402		199.5
	88.50612		25.02372		214.5
	93.54143		26.44738		239.5
	72.74384		20.56718		146.0

Statistical analysis is carried out on the pressure drop data measured from the experiments and the pressure drop characteristics is demonstrated in figure 6. The correlation expression of total pressure drop in terms of velocity at the test section is Δp=-7.62191+0.27637V^2+2.1048V . The regression polynomial indicates reasonable quadratic relationship between the pressure drop and the velocity. The R-Squared value of the regression model is 0.996, which suggests that the confidence level of the correlation expression is high.

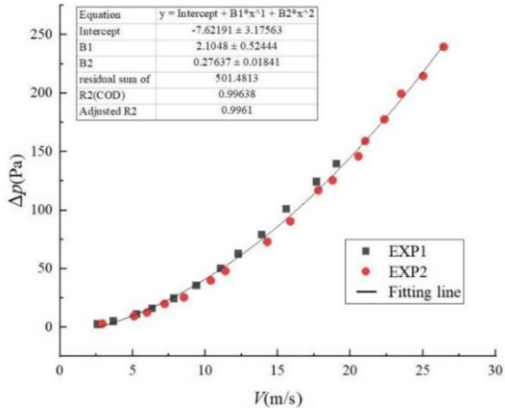

Figure 6. The fitting line of the pressure drop characteristics measured from experiments.

4.2. Pressure Drop Characteristics in Numerical Simulations

It is shown in figure 7 that the pressure drop variations with the velocity both have quadratic patterns in experiments and numerical simulations. However, the gap between experimental and numerical results is growing as the pressure loss increasing since the numerical simulations tends to overpredict the turbulence intensity enhancement as the fluid passing through the screen. The gap between the results from two different experiments also increases as the pressure loss increasing since the measuring errors of the testing devices are magnified by the increase in velocity. The pressure drop measured in EXP1 is slightly higher than that measured in EXP2. The pressure drop is less than 300Pa and the gap between different results is less than 10Pa when the velocity is smaller than 10m/s.

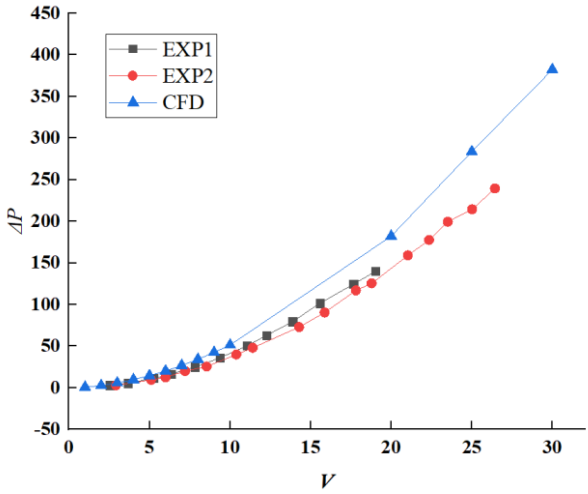

Figure 7. Comparison between the pressure drop characteristics obtained from experiments and numerical simulations.

4.3. Flow Field Analysis

The numerical simulations of the flow field analysis are conduct under the condition of the inlet velocity being equal to 30m/s. Figure 8 shows the pressure distributions on the middle plane and the quarter plane of the computational domain. There is around 1000Pa pressure loss across the wire since there are stagnation points in the back area between the parallel horizonal wires as well as small vortices pairs forming near the intersections of wires that dissipates the fluid energy. Moreover, there is a small area of back flow region just downstream of the wire intersections, as shown in figure 9 where the pressure is slightly higher than the surrounding recirculation regions. The pressure drop in the quarter plane is much smaller than in the middle plane since stagnation only occurs after the obstruction of three horizonal wires. The pressure values change sharply in a short distance near the screen, while the pressure distribution is quite uniform in the other regions of the computational domain.

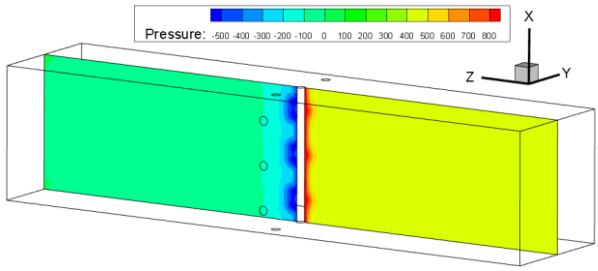

(a)

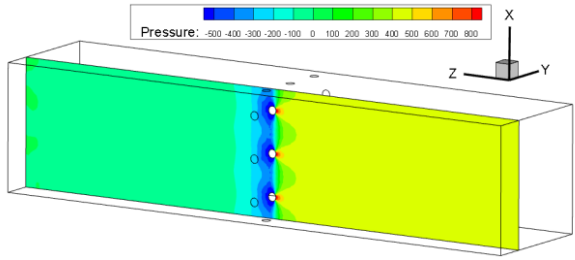

(b)

Figure 8. Pressure distributions in the X-Z planes: (a) the plane is cutting through the central wire; (b) the plane is in the vicinity of the lateral wire.

Figure 10 shows the velocity magnitude distributions as well as streamline distributions on the middle plane and the quarter plane of the computational domain. Figure 9 shows the velocity vector distributions on the middle plane of the computational domain. The velocity magnitude is quite low both behind and in front of the wires due to fluid stagnation and the velocity magnitude is extremely low in the recirculation regions downstream of the wires. It can be observed in the quarter plane that the fluid will speed up between the parallel wires. The velocity distribution becomes uniform again as the fluid leaving away from the screen. The significant velocity magnitude difference between the downstream regions of the apertures and the interwoven wires will lead to strong fluid momentum transport, which also brings about pressure loss.

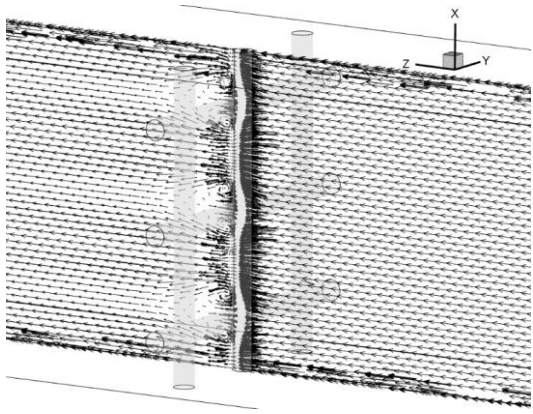

Figure 9. Velocity vector distribution in the X-Z plane.

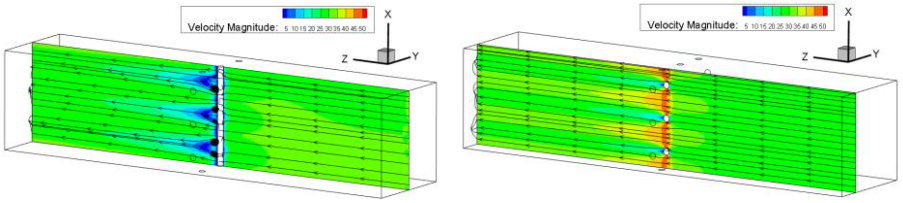

(a) (b)

Figure 10. Streamline distributions superimposed on velocity magnitude contours in the X-Z planes: (a) the plane is cutting through the central wire; (b) the plane is cutting through the lateral wire.

5. Conclusions

This paper experimentally and numerically studied the pressure drop characteristics of a metal mesh screen that blocks the foreign solid matters away from the gas turbine compressor. Compared to the experimental data, the numerical simulations tend to overpredict the turbulence level and then the pressure drop across the screen and the gap between the numerical and experimental results gets larger as the pressure drop increasing. A quadratic polynomial describing the relationship between the pressure drop across the screen and the local velocity is obtained by conducting regression analysis on the experimental data: Δp=-7.62191+0.27637V^2+2.1048V . The flow field analysis indicates that the pressure closely upstream of the wires can be elevated to as high as 4 times of the inlet flow level and a large area of negative pressure regions can be observed downstream of the wires, hence the pressure difference in front of and behind the wires is significantly large. Moreover, backflow and recirculation are observed downstream the intersections of the circular wires, which is the main source of pressure loss.

References

[1] Brekke O and Bakken L E 2010 Performance deterioration of intake air filters for gas turbines in offshore installations *ASME Turbo Expo 2010: Power for Land, Sea, and Air (Glasgow)* vol 5 p 685.
[2] El-Dessouky H T, Alatiqi I M, Ettouney H M and Al-Deffeeri N S 2000 Performance of wire mesh mist eliminator *Chem. Eng. Process.* **39** 129.
[3] Helsør T and Svendsen H 2007 Experimental characterization of pressure drop in dry demisters at low and elevated pressures *Chem. Eng. Res. Des.* **85** 377.
[4] Rahimi R and Abbaspour D 2008 Determination of pressure drop in wire mesh mist eliminator by CFD *Chem. Eng. Process.* **47** 1504.
[5] Setekleiv A E and Svendsen H F 2012 Operation and dynamic behavior of wire mesh pads *Chem. Eng. Sci.* **68** 624.
[6] Janajreh I, Hasania A and Fath H 2013 Numerical simulation of vapor flow and pressure drop across the *demister* of MSF desalination plant *Energy Conv. Manag.* **65** 793.
[7] Sun H, Bu S and Luan Y 2015 A high-precision method for calculating the pressure drop across wire mesh filters *Chem. Eng. Sci.* **127** 143.
[8] Setekleiv A E and Svendsen H F 2016 Dry pressure drop in spiral wound wire mesh pads at low and elevated pressures *Chem. Eng. Res. Des.* **109** 141.
[9] Bussière W, Rochette D, Clain S, André P and Renard J B 2017 Pressure drop measurements for woven metal mesh screens used in electrical safety switchgears *Int. J. Heat Fluid Flow* **65** 60.
[10] Okolo P N, Zhao K, Kennedy J and Bennett G J 2019 Numerical assessment of flow control capabilities of three dimensional woven wire mesh screens *Eur. J. Mech. B-Fluids* **76** 259.
[11] Azizi F 2019 On the pressure drop of fluids through woven screen meshes *Chem. Eng. Sci.* **207** 464.
[12] Wang Y, Yang G, Huang Y, Huang Y, Zhuan R and Wu J 2021 Analytical model of flow-through-

screen pressure drop for metal wire screens considering the effects of pore structures *Chem. Eng. Sci.* **229** 116037.

[13] Abou-Hweij W and Azizi F 2020 CFD simulation of wall-bounded laminar flow through screens. Part I: Hydrodynamic characterization *Eur. J. Mech. B-Fluids* **84** 207.